INORGANIC CHEMISTRY
FRONTIERS

RESEARCH ARTICLE

View Article Online
View Journal | View Issue

Cite this: *Inorg. Chem. Front.*, 2024, **11**, 3548

Strain-based design, direct macrocyclization, and metal complexation of thiazole-containing calix[3]pyrrole analogues†

Keita Watanabe,[a] Kotaro Shibata,[a] Tomoya Ichino,*[b] Yuki Ide,[b] Tomoki Yoneda,[a] Satoshi Maeda[b,c] and Yasuhide Inokuma*[a,b]

The coordination chemistry of ring-contracted porphyrinoids, such as subporphyrins and calix[3]pyrroles, has been largely unexplored owing to the synthetic difficulty of their free-base analogues. Here, we report strain-based molecular design and high-yield synthesis of thiazole-containing calix[3]pyrrole analogues for metal complexation. The artificial force induced reaction and StrainViz analysis methods were used to perform a conformational search and evaluate/visualize the ring strain. The results indicated that the thiazole-containing analogues are less strained than the parent calix[3]pyrrole, while incorporation of imidazole or oxazole unexpectedly leads to an increase in the total strain. Calix[1]furan[2]thiazole was obtained in 60% yield by the direct macrocyclization between α-bromoketone and bis(thioamide), whereas the *meso*-N(sp^2)-bridged analogue, which was calculated to be 5.1 kcal mol^{-1} more strained, was only obtained in a 2% yield. Calix[1]furan[2]thiazole was converted to calix[1]pyrrole[2]thiazole to investigate metal complexation. Through the reaction with Et_2Zn, calix[1]pyrrole[2]thiazole bound a Zn(II) ion in a tridentate fashion adopting a cone conformation, giving a water/air stable organozinc complex that catalyzes polymerization of lactide. Conversely, Ag(I) and Pd(II) ions coordinated to the partial cone conformation of calix[1]pyrrole[2]thiazole in a bidentate fashion. Strain-based molecular design expands the synthetic access to contracted porphyrinoids and provides the opportunity to take advantage of their rich coordination chemistry.

Received 17th March 2024,
Accepted 3rd May 2024

DOI: 10.1039/d4qi00684d

rsc.li/frontiers-inorganic

Introduction

Contracted porphyrins, such as subphthalocyanines and subporphyrins, have recently attracted much attention owing to their bowl-shaped structures, 14π-aromatic characters, and visible absorption/emission properties.[1–3] Since the discovery of boron(III)–subphthalocyanine by Meller and Ossko in 1972,[4] boron-templated synthesis has played a central role in developing their analogues by core modification and peripheral functionalization.[5] The boron template is almost essential for the synthesis of triphyrin(1.1.1)-type contracted porphyrinoids, because the boron-free analogues have not yet been obtained from the direct macrocyclization of pyrrole monomers. While most subphthalocyanines and subporphyrins are obtained as boron(III)-complexes, removal of the boron atom remains unsuccessful. The unavailability of boron-free contracted porphyrins has hampered the development of their coordination chemistry, although metal complexation has endowed other porphyrinoids with various properties, such as catalysis,[6] photosensitization,[7] and coordination-driven self-assembly.[8]

Recent advances have demonstrated that boron-free subporphyrin[9] and calix[3]pyrrole (**1**),[10] a porphyrinogen-type congener of subporphyrin, stably exist without any template atoms, which has provided the opportunity to explore their metal complexes. However, the low synthetic yields of the free-base analogues still hinder further investigations. Suzuki–Miyaura cross coupling gives the subporphyrin free-base only in 4% yield, and synthesis of **1** requires five steps from a commercial precursor with a total yield of 4%. Simple, high-yield synthetic routes for boron-free contracted porphyrinoids are still being pursued in this research area.

Recent studies have suggested that the synthetic difficulty arises from the unusual increase in the ring strain during the formation of tripyrrolic macrocycles from linear precursors.[11] Although synthetic and theoretical evaluation of the calix[*n*]

[a]*Division of Applied Chemistry, Faculty of Engineering, Hokkaido University, Kita 13, Nishi 8, Kita-ku, Sapporo, Hokkaido, 060-8628, Japan. E-mail: inokuma@eng.hokudai.ac.jp*
[b]*Institute for Chemical Reaction Design and Discovery (WPI-ICReDD), Hokkaido University, Kita-21, Nishi 10, Kita-ku, Sapporo, Hokkaido, 001-0021, Japan. E-mail: tichino@eis.hokudai.ac.jp*
[c]*Department of Chemistry, Faculty of Science, Hokkaido University, Kita 10, Nishi 8, Kita-ku, Sapporo, Hokkaido, 060-8610, Japan*

†Electronic supplementary information (ESI) available. CCDC 2326011–2326017. For ESI and crystallographic data in CIF or other electronic format see DOI: https://doi.org/10.1039/d4qi00684d

furan[3 − *n*]pyrrole (*n* = 0–3) system indicates that the ring strain increases as the number of NH units increases, the relationship between the ring strain and synthetic accessibility is still unclear. Here, we report the strain-based molecular design and efficient synthesis of thiazole-containing, boron-free calix[3]pyrrole analogues, calix[1]pyrrole[2]thiazole (**2**) and calix[1]furan[2]thiazole (**5**), as well as the derivatization of **2** to metal complexes. For the design of less-strained macrocycles, we used the Artificial Force Induced Reaction (AFIR)[12] method-based conformational search and visualization of the macrocyclic ring strain using the StrainViz analysis,[13] which was developed by Justi and co-workers for the evaluation of the strain of cycloparaphenylenes. Contrary to our semi-empirical expectation, replacement of two pyrrole units in calix[3]pyrrole **1** with oxazole or imidazole rings resulted in a significant increase in the total strain, while the thiazole-containing analogues were less strained. The validity of the theoretical expectations was confirmed through the synthesis of **5** and its *meso*-N(sp^2)-bridged analogue **10**. While **5** was obtained in 60% yield, **10**, which was calculated to be 5.1 kcal mol^{-1} more strained, was only obtained in 2% yield. Calix[3]pyrrole-related ligand **2** switched its conformation between the partial cone and the cone to chelate various metal ions to provide a moisture-stable organozinc catalyst for *rac*-lactide polymerization and coordination assembly, demonstrating the unique coordination chemistry of the contracted calixpyrrole.

Results and discussion

To design a less-strained calix[3]pyrrole analogue for metal complexation, we theoretically evaluated several heteroarene-embedded macrocycles **2–5** (see the ESI† for the computational details). On the basis of the semi-empirical trends obtained for calix[*n*]furan[3 − *n*]pyrrole, we expected that replacing the two pyrrole units in **1** with thiazole, imidazole, or oxazole rings would reduce the total strain owing to the decreasing number of inner NH protons, since the strain-induced ring expansion reaction occurred for *n* = 0 and 1, but not for *n* = 2, 3. Furthermore, the iminic nitrogen atoms in these heteroarenes would contribute to form metal complexes. To evaluate the ring strain, the lowest energy conformations of **1–5** were obtained by a searched using the AFIR method, and they were further optimized by the density functional theory (DFT) calculations at the M06-2X/6-311+G(2d,p) level (Fig. 1a). The optimized structure of calix[3]pyrrole (**1**) adopted a partial cone conformation, as observed in its crystal structure. The dihedral strain (11.7 kcal mol^{-1}) greatly contributed to the total strain of 13.4 kcal mol^{-1} (Fig. 1c). The StrainViz analysis revealed that the C(pyrrole-α)–C(*meso*) bond had the maximum strain (Fig. 1b). Calix[1]pyrrole[2]thiazole (**2**) exhibited a cone conformation with a NH···N distance of 2.11 Å, and the dihedral strain was significantly reduced compared with that of **1**. The total strain of **2** was 2.9 kcal mol^{-1} lower than that of **1**, suggesting that **2** is more easily accessible. Contrary to our empirical expectation, the lowest energy conformation of imidazole derivative **3** had three inner NH protons (Fig. S4†). Because of the increased dihedral strain, the total strain of **3** was 2.2 kcal mol^{-1} larger than that of **1**. Although oxazole derivative **4** showed a cone conformation similar to that of **2**, the total strain was comparable to that of **3** owing to the large contribution of the dihedral strain around the C(*meso*)–C(pyrrole-α) bonds. When the pyrrole unit in the less-strained **2** was replaced with furan, the angle strain was reduced by 0.6 kcal mol^{-1}, but the dihedral strain increased by 1.0 kcal mol^{-1}, resulting in **2** and **5** having similar total strain energies. According to the theoretical calculations, thiazole-containing derivatives **2** and **5** are the most feasible among the evaluated compounds **1–5**. Given the synthetic availability of furan precursor **6**,[14] we investigated direct macrocyclization synthesis of **5** using a Hantzsch-type thiazole formation reaction.[15]

To our delight, the condensation reaction between **6** and 2,2-dimethylpropanebis(thioamide) (**7**)[16] in refluxing ethanol gave calix[1]furan[2]thiazole (**5**) in 60% yield (Scheme 1), along with a double sized macrocycle, calix[2]furan[4]thiazole, in 16% yield (compound **14** in ESI†). The ^{1}H NMR spectrum of **5** in $CDCl_3$ showed time-averaged C_{2v} molecular symmetry, featuring four singlet signals at 6.78, 5.88, 1.93, and 1.63 ppm assignable to thiazole, furan and two different methyl protons, respectively.

Although strained calix[3]pyrrole analogues typically undergo strain-induced ring expansion reactions under acidic conditions,[11] macrocycle **5** was sufficiently stable to exist in the presence of trifluoroacetic acid (TFA) in CH_2Cl_2. Vapor diffusion of hexane into a dichloromethane/TFA solution of **5** gave single crystals of the protonated form **5**·TFA (Fig. 2). X-ray diffraction analysis revealed that **5**·TFA adopted a cone conformation that is commonly observed for less-strained calix[3]pyrrole analogues.[10] The C–N–C bond angles of the thiazole units were 116.9° and 112.5°, indicating that the former was the *N*-protonated moiety.

When **5** was treated with aqueous hydrochloric acid, the furan moiety was hydrolyzed to give 1,4-diketone-linked macrocycle **8** quantitatively. The Paal–Knorr reaction of **8** with ammonium acetate gave calix[1]pyrrole[2]thiazole (**2**) in 78% yield. The total yield of **2** from the known precursors was 30% in three steps, which is markedly higher than those reported for **1** and the subporphyrin free-base. The ^{1}H NMR spectrum of **2** recorded in $CDCl_3$ also exhibited a C_{2v}-symmetric signal pattern. The NH proton was observed at 12.17 ppm, indicating a hydrogen bond with the thiazole units. Similar to **5**, macrocycle **2** did not undergo a strain-induced ring expansion reaction under standard conditions using TFA.[11] Single crystal X-ray diffraction analysis confirmed that **2** had a cone conformation, which was predicted by an AFIR-based conformational search. The N(thiazole)–N(thiazole) and N(pyrrole)–N(thiazole) distances were 2.820 and 2.702 Å, respectively, suggesting the potential for the cooperative coordination of metal ions using three nitrogen atoms.

The significance of evaluating the ring strain before conducting a synthetic examination was demonstrated by the syn-

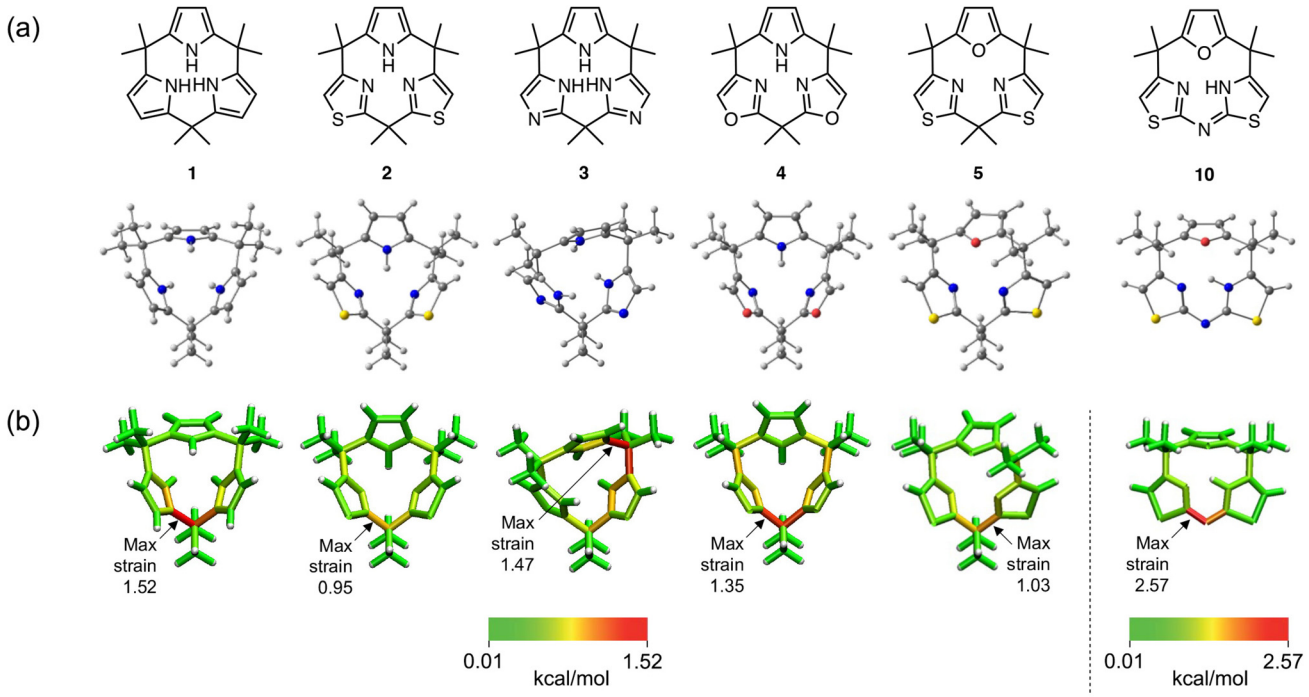

(c)

Compound	1	2	3	4	5	10
Total strain	13.4	10.5	15.6	15.5	10.7	15.8
Bond strain	0.5	0.5	0.5	0.7	0.5	2.3
Angle strain	1.1	1.8	1.3	1.9	1.2	5.4
Dihedral strain	11.7	8.1	13.8	12.9	9.1	8.0

(energy in kcal/mol)

Fig. 1 (a) Optimized structures of the lowest energy conformations of calix[3]pyrrole (**1**) and its analogues **2**–**5**, and **10**. (b) Visualization of the total ring strain of **1**–**5** and **10** using the StrainViz analysis. (c) Calculated total, bond, angle, and dihedral strain energies of **1**–**5** and **10** (in kcal mol^{-1}).

thesis of *meso*-N(sp^2)-bridged analogue **10**. An AFIR-based conformational search revealed that the most stable conformation of **10** is an uncommon gable-like conformation, in which the *N*-bridged bis(thiazole) unit is almost planar, but the total strain (15.8 kcal mol^{-1}) is the largest of the series of molecules (Fig. 1). Despite our tremendous efforts, reaction between **7** and **9** gave only a trace amount (2% yield) of the target **10** (Scheme 1), while a calix[6]-type macrocycle was obtained in 32% yield along with other oligomeric products (compound **15** in ESI†). Single crystal X-ray analysis also showed the gable-like conformation of **10** (Fig. 2c). Through the imine–enamine tautomerism, the *meso*-N atom lost a hydrogen atom, resulting in the formation of an inner NH group. Owing to the intramolecular hydrogen-bonding interaction, the inner NH proton was observed at 18.67 ppm in the ^{1}H NMR spectrum recorded in $CDCl_3$. These results demonstrated that the AFIR method is useful for searching for the stable conformations, and the comparison of the calculated total strains can indicate the synthetic feasibility of calix[3]pyrrole derivatives.

In our previous report, we found that absorption spectra of calix[3]pyrrole analogues show characteristically red-shifted absorption as a result of strained ring system.[17] Compounds **2** and **5** also exhibited similar broad bands around 300 nm in dichloromethane (Fig. S26†). In the case of N(sp^2)-linked **10**, a strong absorption band with absorption coefficient of $\varepsilon = 1.9 \times 10^4$ M^{-1} cm^{-1} was observed at 339 nm, showing the effect of π-conjugation through the *meso*-N atom.

The reliable synthetic route of **2** allowed further investigation of its coordination chemistry. Among porphyrin-related ligands, calix[4]pyrroles, a parent tetrapyrrolic macrocycle of **1**, have shown their unique metal binding behavior. Depending on the metal ions, calix[4]pyrroles can switch their conformations and the coordination mode of each pyrrole unit from η^1- to η^5-manners.[18] After several attempts using various metal salts, we found that Et_2Zn, $Pd(MeCN)_4(BF_4)_2$, and $AgBF_4$ can form isolable metal complexes with **2**.

When **2** was treated with diethylzinc in dry toluene, ethyl zinc complex **11** was obtained as a yellow crystalline solid in 72% yield (Fig. 3). ^{1}H NMR spectroscopy of **11** confirmed that the pyrrole NH proton disappeared, while the ethyl proton signals were observed at 0.54(q) and 1.37(t) ppm. The single crystal X-ray structure of **11** showed a cone-shaped confor-

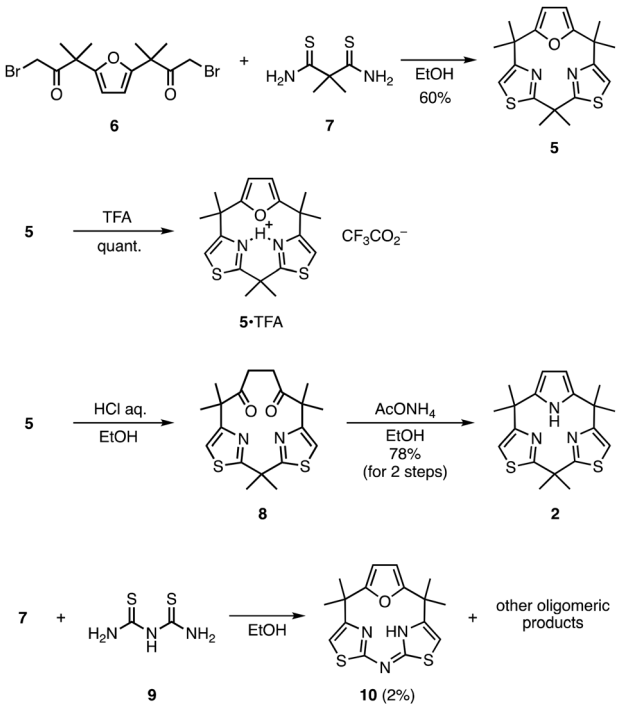

Scheme 1 Synthesis of thiazole-containing calix[3]pyrrole analogues.

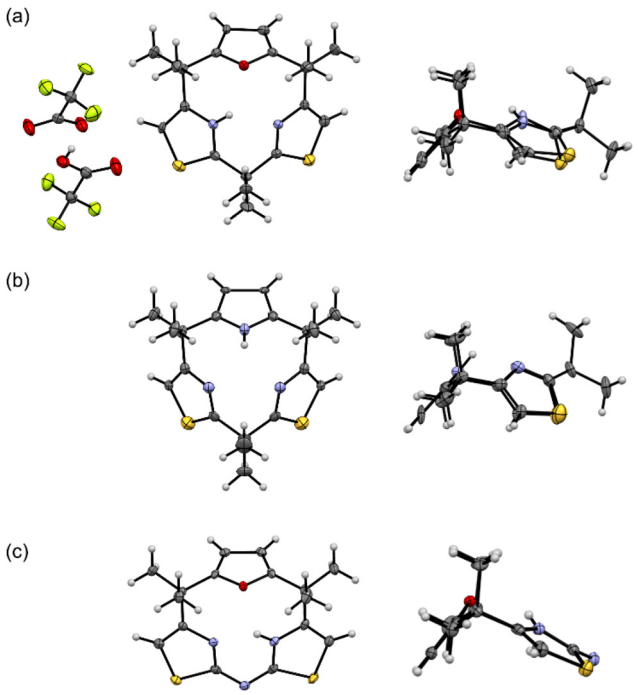

Fig. 2 Single crystal X-ray structures (left, top view; right, side view) of (a) **5**·TFA, (b) **2**, and (c) **10** drawn at the 50% probability level of the thermal ellipsoids (H, white; C, gray; N, blue; O, red; S, yellow; and F, yellow green).

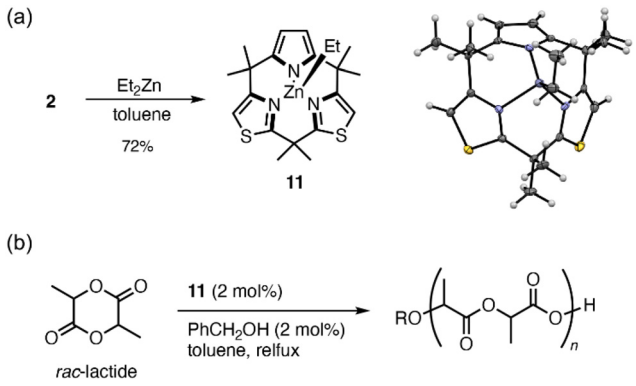

Fig. 3 (a) Synthesis and crystal structure of organozinc complex **11**. (b) Polymerization of *rac*-lactide catalyzed by **11**.

mation of the ligand that chelated to the ethyl Zn(II) moiety in a monoanionic tridentate manner. Because three *meso*-Me substituents were located in an almost perpendicular fashion to the macrocycle, the zinc center was sterically protected by the ligand. The UV-vis absorption spectrum of **11** showed that the absorption bands of ligand **2** were slightly red-shifted with broadening upon zinc complexation (Fig. S26†).

Organozinc complex **11** showed remarkable stability toward water, alcohol, and air at room temperature, and it can thus be treated in organic solutions without special care.[19] When complex **11** was dissolved in wet $CDCl_3$ at 13 mM (containing ≥5.0 equiv. of H_2O), hydrolysis was not observed after 1 h at room temperature by ^1H NMR spectroscopy, while diethylzinc was immediately decomposed under similar conditions. Similar tests with ≥70 equiv. of methanol, ethanol, and isopropyl alcohol exhibited recovery of ≥97% of **11** after 1 h (Fig. S21†). Whereas, addition of more acidic phenol or benzoic acid (3.0 equiv.) resulted in the considerable demetallation of **11** to give **2**. Air oxidation of **11** was not observed after standing a chloroform solution of **11** or the crystalline solids in an aerobic atmosphere for more than 2 days.

Organozinc complex **11** is sufficiently stable to be handled under non-dried aerobic conditions, and it shows catalytic activity for the polymerization of *rac*-lactide.[20] When a toluene solution of *rac*-lactide was heated to reflux in the presence of **11** and benzyl alcohol (2 mol% each), >95% of the monomer was converted in 30 min to give poly(lactide) with number-average molecular weight of 9.0 kg mol^{-1} and polydispersity index of 1.4.

Upon complexation with $Pd(MeCN)_4(BF_4)_2$, macrocycle **2** formed cationic Pd(II) complex **12** adopting a partial cone conformation (Fig. 4). The quantitative complexation behavior was monitored by ^1H NMR spectroscopy (Fig. S23†). Upon addition of the Pd(II) salt to a CD_3CN solution of **2** at 5.6 mM, new signals assignable to the thiazole and pyrrole protons of **12** appeared at 7.68 and 6.72 ppm, respectively. After the addition of 1.0 equiv. of the salt, the signals of **2** were almost converted to those of **12**, indicating its quantitative formation. Vapor diffusion of diethyl ether into an acetonitrile solution of **12** gave diffraction grade single crystals. Crystallographic analysis revealed a partial cone conformation of **12** in which ligand **2** coordinated to the Pd(II) ion in a square planar coordination

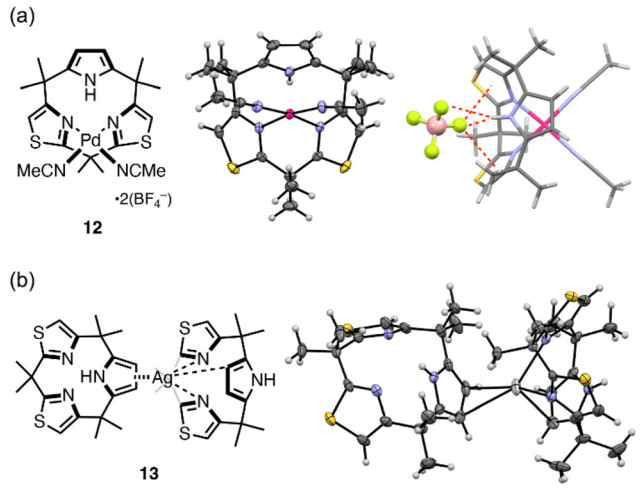

Fig. 4 Transition metal complexes of ligand **2** with partial cone conformations. (a) Chemical structure (left), ORTEP drawing of the crystal structure (center), and anion binding mode in the solid state (right) of Pd-complex **12**. (b) Chemical structure (left) and ORTEP drawing (right) of Ag(I)-linked coordination assembly **13**.

geometry with two thiazole nitrogen atoms, leaving the pyrrole unit uncoordinated. The pyrrole NH site was hydrogen bonded to a BF_4 anion, which was also in a close proximity to two thiazole planes. NCI plot analysis[21] suggested that weak but non-trivial anion–π interactions existed between the BF_4 anion and thiazole moieties (Fig. S18†). Although such anion binding behavior was not observed in solution, these observations indicated the unique structural and supramolecular properties of calix[3]pyrrole-related ligand **2**.

Complexation with $AgBF_4$ also gave a coordination assembly of **2**. ^{1}H NMR titration of **2** with the Ag(I) salt in CD_3CN exhibited a gradual shift of the proton signals due to **2**, indicating reversible metal coordination with a rapid exchanging rate on the NMR time scale. Job's plot analysis indicated a 1 : 1 complexation of **2** with Ag(I) ions in solution at ~10 mM concentration (Fig. S24†). However, when single crystals of the Ag(I)-complex were grown from the solution, Ag(I)-linked dyad **13** was obtained (Fig. 4). Complex **13** was composed of an Ag(I) ion and two ligands **2** in different conformations. The ligand **2** in the partial cone conformation coordinated to the Ag(I) ion using two N(thiazole) atoms in a similar fashion to **12**, while the Ag–C(pyrrole-β) distance of 2.66 Å indicated coordination of the pyrrole unit in an η^1 fashion. The other ligand **2** in the cone conformation chelated to the Ag(I) ion with η^2-pyrrole–Ag(I) coordination bonds, leaving the thiazole units uncoordinated. When the crystals of **13** were dissolved in CD_3CN, the ^{1}H NMR spectrum of an equilibrated solution, which was also observed during titration with Ag(I), was obtained due to the reversible metal coordination. Nevertheless, the formation of complex **13** demonstrated the possibility of coordination self-assembly of **2**, which can be used as the principal interactions to construct giant supramolecules.

Conclusions

In conclusion, a conformational search and strain visualization using the AFIR and StrainViz methods allowed the rational design of less-strained thiazole-containing calix[3]pyrrole analogues, **2** and **5**. The total strain energy and synthetic yield were found to be almost inversely proportional. Hence, strain calculations are more important than semi-empirical design for considering the feasible synthetic targets. The scalable synthetic route for **2** enabled investigation of metal complexes of the calix[3]pyrrole-type ligand. Formation of the moisture-stable organozinc complex **11** demonstrated the unique properties of ligand **2** that can protect the metal center within the narrow cavity. Complexation with Pd(II) and Ag(I) ions showed the conformational flexibility of **2** during metal coordination and the possibility of coordination self-assembly to produce giant supramolecules. The present results will lead to various types of contracted porphyrins without template atoms through strain-based design, allowing further synthetic functionalization and metal complexation. Moreover, as a novel class of ligands, boron-free calix[3]pyrrole-type macrocycles will produce a range of organometallic complexes, metal clusters, and coordination polymers, which will contribute to advance in the field of inorganic chemistry.

Data availability

The ESI contains synthetic procedures, computational details, crystallographic data, and NMR spectra.

Author contributions

Y. Inokuma designed the study, supervised the project, and wrote the first version of the draft. K. W., K. S., Y. Ide, and T. Y. performed experimental work. T. I. and S. M. did computational analyses.

Conflicts of interest

There are no conflicts to declare.

Acknowledgements

This work was partly supported by a JSPS Grant-in-Aid for Scientific Research (B) (No. 22H02058) and JST FOREST Program (No. JPMJFR211H), of which Y. Inokuma is the principal investigator. This work was also partly supported by Toyota Riken Scholar and NOASTEC Foundation to T. Y. The Institute for Chemical Reaction Design and Discovery (ICReDD) was established by World Premier International Research Initiative (WPI), MEXT, Japan.

References

1 G. Lavarda, J. Labella, M. V. Martínez-Díaz, M. S. Rodríguez-Morgade, A. Osuka and T. Torres, Recent advances in subphthalocyanines and related subporphyrinoids, *Chem. Soc. Rev.*, 2022, **51**, 9482–9619.

2 (*a*) C. G. Claessens, D. González-Rodríguez, M. S. Rodríguez-Morgade, A. Medina and T. Torres, Subphthalocyanines, Subporphyrazines, and Subporphyrins: Singular Nonplanar Aromatic Systems, *Chem. Rev.*, 2014, **114**, 2192–2277; (*b*) Y. Inokuma and A. Osuka, Subporphyrins: emerging contracted porphyrins with aromatic 14π-electronic systems and bowl-shaped structures: rational and unexpected synthetic routes, *Dalton Trans.*, 2008, 2517–2526; (*c*) M. Pawlicki and L. Latos-Grażyński, Aromaticity Switching in Porphyrinoids, *Chem. – Asian J.*, 2015, **10**, 1438–1451.

3 (*a*) D. González-Rodríguez, T. Torres, M. M. Olmstead, J. Rivera, M. Á. Herranz, L. Echegoyen, C. A. Castellanos and D. M. Guldi, Photoinduced Charge-Transfer States in Subphthalocyanine-Ferrocene Dyads, *J. Am. Chem. Soc.*, 2006, **128**, 10680–10681; (*b*) S. Shimizu, Recent Advances in Subporphyrins and Triphyrin Analogues: Contracted Porphyrins Comprising Three Pyrrole Rings, *Chem. Rev.*, 2017, **117**, 2730–2784; (*c*) A. Osuka, E. Tsurumaki and T. Tanaka, Subporphyrins: A Legitimate Ring-Contracted Porphyrin with Versatile Electronic and Optical Properties, *Bull. Chem. Soc. Jpn.*, 2011, **84**, 679–697.

4 A. Meller and A. Ossko, Phthalocyaninartige Bor-Komplexe, *Monatsh. Chem.*, 1972, **103**, 150–155.

5 (*a*) C. G. Claessens, D. González-Rodríguez and T. Torres, Subphthalocyanines: Singular Nonplanar Aromatic CompoundsSynthesis, Reactivity, and Physical Properties, *Chem. Rev.*, 2002, **102**, 835–853; (*b*) Y. Inokuma, J. H. Kwon, T. K. Ahn, M.-C. Yoon, D. Kim and A. Osuka, Tribenzosubporphines: Synthesis and Characterization, *Angew. Chem., Int. Ed.*, 2006, **45**, 961–964; (*c*) N. Kobayashi, Y. Takeuchi and A. Matsuda, *meso*-Aryl Subporphyrins, *Angew. Chem., Int. Ed.*, 2007, **46**, 758–760; (*d*) Z. Li, L. Zhang, Q. Wu, H. Li, Z. Kang, C. Yu, E. Hao and L. Jiao, Boron-Templated Synthesis of B(III)-Submonoazaporphyrins: The Hybrids of B(III)-Subporphyrins and B(III)-Subporphyrazines, *J. Am. Chem. Soc.*, 2022, **144**, 6692–6697.

6 (*a*) B. Meunier, Metalloporphyrins as versatile catalysts for oxidation reactions and oxidative DNA cleavage, *Chem. Rev.*, 1992, **92**, 1411–1456; (*b*) S. Fukuzumi, Y.-M. Lee and W. Nam, Mechanisms of Two-Electron versus Four-Electron Reduction of Dioxygen Catalyzed by Earth-Abundant Metal Complexes, *ChemCatChem*, 2018, **10**, 9–28; (*c*) C.-M. Che, V. K.-Y. Lo, C.-Y. Zhou and J.-S. Huang, Selective functionalisation of saturated C–H bonds with metalloporphyrincatalysts, *Chem. Soc. Rev.*, 2011, **40**, 1950–1975; (*d*) L. Feng, K.-Y. Wang, E. Joseph and H.-C. Zhou, Catalytic Porphyrin Framework Compounds, *Trends Chem.*, 2020, 555–568.

7 (*a*) J. R. Darwent, P. Douglas, A. Harriman, G. Porter and M.-C. Richoux, Metal phthalocyanines and porphyrins as photosensitizers for reduction of water to hydrogen, *Coord. Chem. Rev.*, 1982, **44**, 83–126; (*b*) R. Bonnet, Photosensitizers of the porphyrin and phthalocyanine series for photodynamic therapy, *Chem. Soc. Rev.*, 1995, **24**, 19–33; (*c*) J. Karges, Clinical Development of Metal Complexes as Photosensitizers for Photodynamic Therapy of Cancer, *Angew. Chem., Int. Ed.*, 2022, **61**, e202112236; (*d*) A. R. Sekhar, Y. Chitose, J. Janoš, S. I. Dangoor, A. Ramundo, R. Satchi-Fainaro, P. Slavíček, P. Klán and R. Weinstain, Porphyrin as a versatile visible-light-activatable organic/metal hybrid photoremovable protecting group, *Nat. Commun.*, 2022, **13**, 3614.

8 (*a*) I. Beletskaya, V. S. Tyurin, A. Y. Tsivadze, R. Guilard and C. Stern, Supramolecular Chemistry of Metalloporphyrins, *Chem. Rev.*, 2009, **109**, 1659–1713; (*b*) P. S. Bols and H. L. Anderson, Template-Directed Synthesis of Molecular Nanorings and Cages, *Acc. Chem. Res.*, 2018, **51**, 2083–2092; (*c*) X. Chi, A. J. Guerin, R. A. Haycock, C. A. Hunter and L. D. Sarson, Self-assembly of macrocyclic porphyrin oligomers, *J. Chem. Soc., Chem. Commun.*, 1995, **24**, 2567–2569; (*d*) J. A. Faiz, V. Heitz and J.-P. Sauvage, Design and synthesis of porphyrin-containing catenanes and rotaxanes, *Chem. Soc. Rev.*, 2009, **38**, 422–442.

9 L. Liu, J. Kim, L. Xu, Y. Rao, M. Zhou, B. Yin, J. Oh, D. Kim, A. Osuka and J. Song, Synthesis of Subporphyrin Free Bases, *Angew. Chem., Int. Ed.*, 2022, **61**, e202214342.

10 Y. Inaba, Y. Nomata, Y. Ide, J. Pirillo, Y. Hijikata, T. Yoneda, A. Osuka, J. L. Sessler and Y. Inokuma, Calix[3]pyrrole: A Missing Link in Porphyrin-Related Chemistry, *J. Am. Chem. Soc.*, 2021, **143**, 12355–12360.

11 Y. Inaba, Y. Kakibayashi, Y. Ide, J. Pirillo, Y. Hijikata and Y. Inokuma, Strain-Induced Ring Expansion Reactions of Calix[3]pyrrole-Related Macrocycles, *Chem. – Eur. J.*, 2022, **28**, e202200056.

12 (*a*) S. Maeda, K. Ohno and K. Morokuma, Systematic exploration of the mechanism of chemical reactions: the global reaction route mapping (GRRM) strategy using the ADDF and AFIR methods, *Phys. Chem. Chem. Phys.*, 2013, **15**, 3683–3701; (*b*) S. Maeda and Y. Harabuchi, Exploring paths of chemical transformations in molecular and periodic systems: An approach utilizing force, *Wiley Interdiscip. Rev.: Comput. Mol. Sci.*, 2021, **11**, e1538.

13 C. E. Colwell, T. W. Price, T. Stauch and R. Jasti, Strain visualization for strained macrocycles, *Chem. Sci.*, 2020, **11**, 3923–3930.

14 H. Fujita, S. Arai, H. Arakawa, K. Hamamoto, T. Kato, T. Arai, N. Nitta, K. Hotta, N. Hosokawa, T. Ohbayashi, C. Takahashi, Y. Inokuma, I. Tamai, S. Yano, M. Kunishima and Y. Watanabe, Drug–drug conjugates of MEK and Akt inhibitors for RAS-mutant cancers, *Bioorg. Med. Chem.*, 2024, **102**, 117674.

15 A. Hantzsch and J. H. Weber, Ueber Verbindungen des Thiazols (Pyridins der Thiophenreihe), *Ber. Dtsch. Chem. Ges.*, 1887, **20**, 3118.

16 S. H. J. D. Beuleleer and H. O. Desseyn, Thermal analysis of dithiomalonoamide complexes, *J. Therm. Anal.*, 1996, **47**, 135–142.

17 K. Watanabe, R. Saha, Y. Inaba, Y. Manabe, T. Yoneda, Y. Ide, Y. Hijikata and Y. Inokuma, Absorption Spectra of Calix[3]pyrrole Analogues as Probes for Contracted Macrocycles, *J. Porphyrins Phthalocyanines*, 2023, **27**, 157–163.

18 H. Ruppert, L. M. Sigmund and L. Greb, Calix[4]pyrroles as ligands: recent progress with a focus on the emerging p-block element chemistry, *Chem. Commun.*, 2021, **57**, 11751.

19 H. Irving and R. J. P. Williams, The stability of transition-metal complexes, *J. Chem. Soc.*, 1953, 3192–3210.

20 (*a*) O. Dechy-Cabaret, B. Martin-Vaca and D. Bourissou, Controlled Ring-Opening Polymerization of Lactide and Glycolide, *Chem. Rev.*, 2004, **104**, 6147–6176; (*b*) R. Petrus and P. Sobota, Magnesium and zinc alkoxides and aryloxides supported by commercially available ligands as promoters of chemical transformations of lactic acid derivatives to industrially important fine chemicals, *Coord. Chem. Rev.*, 2019, **396**, 72–88; (*c*) G. Sachdeva, Y. Bamal, A. Ladan, O. S. Tiwari, V. Rawat, P. Yadav and V. P. Verma, Calixarene-Metal Complexes in Lactide Polymerization: The Story so Far, *ACS Omega*, 2023, **8**, 13479–13491.

21 J. Contreras-García, E. R. Johnson, S. Keinan, R. Chaudret, J.-P. Piquemal, D. N. Beratan and W. Yang, NCIPLOT: A Program for Plotting Noncovalent Interaction Regions, *J. Chem. Theory Comput.*, 2011, **7**, 625–632.